

## 20000G shock energy harvesters for gun-fired munition

**J. Willemin<sup>1,2</sup>, S. Boisseau<sup>1,2</sup>, L. Olmos<sup>1,2</sup>, M. Gallardo<sup>1,2</sup>, G. Despesse<sup>1,2</sup>, T. Robert<sup>3</sup>**

<sup>1</sup> Univ. Grenoble Alpes, F-38000 Grenoble, France

<sup>2</sup> CEA, Leti, Minatec Campus, 17 rue des Martyrs - 38054 Grenoble Cedex 9, France

<sup>3</sup> Nexter Munitions, La Chapelle, Route de Villeneuve - 18570 La Chapelle Saint Ursin, France

E-mail: jerome.willemin@cea.fr

**Abstract.** This paper presents a 20000G shock energy harvester dedicated to gun-fired munitions and based on a mass-spring resonant structure coupled to a coil-magnet electromagnetic converter. The 20000G shock energy is firstly stored in the spring as elastic potential energy, released as mass-spring mechanical oscillations right after the shock and finally converted into electricity thanks to the coil-magnet transducer. The device has been modeled, sized to generate 200mJ in 150ms, manufactured and tested in a gun-fired munition. The prototype sizes 117cm<sup>3</sup> and weighs 370g. 210mJ have been generated in a test bench and 140mJ in real conditions; this corresponds to a mean output power of 0.93W (7.9mW/cm<sup>3</sup>) and a maximum output power of 4.83W (41.3mW/cm<sup>3</sup>) right after the shock.

### 1. Introduction - Shock energy harvester concept

The use of electromagnetic converters in energy harvesters dates back to the beginning of the energy harvesting era. Yet, they still offer great innovation and optimization opportunities in various fields such as biomechanical energy harvesting [1], water flow energy harvesting [2] or high-G shock energy harvesting, which is the topic of this paper. The concept of the energy harvesters proposed here is close to the one developed by Rastegar et al. [3-4]; but, because of cost issues, the choice has been made to use an electromagnetic converter instead of a piezoelectric one. The basic concept of our high-G energy harvesters is presented in Figure 1a: during the firing phase, the energy harvester is subjected to a 20000G acceleration, the mass is projected towards the bottom of the device and elastic potential energy is stored in the spring. Right after the shock, this potential energy is released as mechanical oscillations (mass-spring) which are eventually converted into electricity thanks to a coil-magnet transducer. The use of mechanical oscillations enables to convert energy in several periods, which has the great benefit of limiting the size of the electromagnetic transducer. The acceleration as a function of time of the shock to harvest is presented in Figure 1b: the shock lasts  $T_{\text{shock}} \approx 10\text{ms}$  and reaches exactly 22700G at  $t \approx 5\text{ms}$ .

### 2. Shock energy harvester – models and equations

The energy harvester's model is presented in Figure 2a. The mechanical part is a mass-spring resonator damped by mechanical ( $b_m$ ) and electrical forces; the electric part a coil-resistor circuit. This energy harvester is ruled by the system of equation presented in Figure 2b, deduced from Newton's second law and Kirchhoff's laws, where  $m$  is the mobile mass,  $k$ , the spring stiffness,  $b_m$ , the mechanical damping ratio,  $z(t)$ , the mass position,  $Bl$ , the electromechanical coupling of the coil-magnet converter,



$L$ , the coil inductance,  $r_l$ , the coil resistance and  $R$ , the load. The energy harvester can be modeled by an equivalent electric circuit with a mechanical and an electric part (Figure 2c) [5-6]. The electromechanical coupling is modelled by a transformer with a  $Bl:Bl$  conversion ratio and with  $\dot{z}$  flowing on the primary and  $i$  on the secondary.

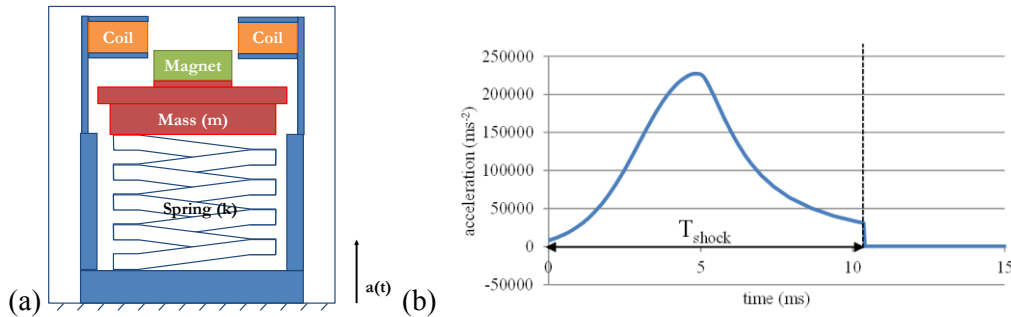


**Figure 1.** (a) Energy harvester concept and (b) Shock to harvest

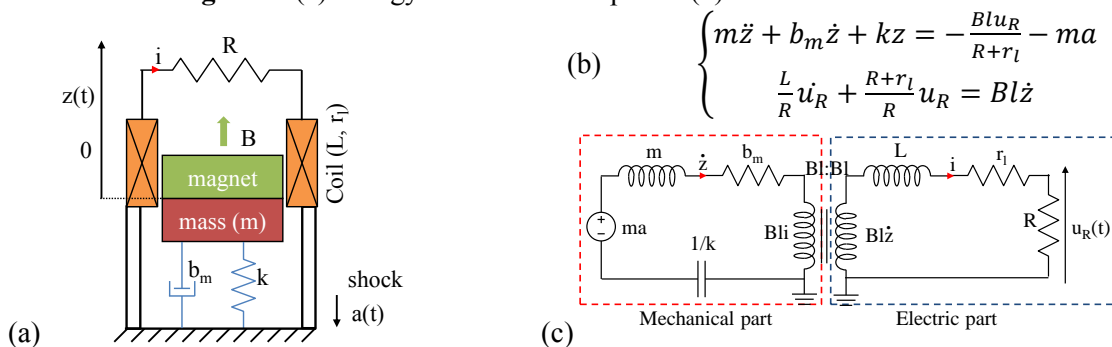


**Figure 2.** (a) Energy harvester model, (b) system of differential equations ruling the energy harvester's behavior, and (c) equivalent electric model

### 3. Simulations and energy harvester conception

#### 3.1. Parameters and simulated output energies

The energy harvester's equations have been implemented in Matlab/Simulink to determine the parameters maximizing the output energy. The time acceleration (Figure 1b) is directly used as the input excitation; the output energy targeted is  $E=200\text{mJ}$  in  $150\text{ms}$ . The most important parameter is the resonant frequency of the mass-spring system ( $f_{mk}$ ). Actually, so as to ensure the mechanical oscillations, the  $20000\text{G}$  acceleration must be perceived as a shock by the mass-spring resonator. Then  $T_{mk}=1/f_{mk}$ , the mechanical period of the mass-spring oscillator, must be small compared to  $T_{shock}$ ; then, on the one hand,  $f_{mk} \gg 100\text{Hz}$ . On the other hand,  $f_{mk}$  should be small enough to induce a sufficient oscillation amplitude  $z$ . Simulations have been performed and have shown that the output energy is maximized for  $f_{mk}=299\text{Hz}$ . The maximum displacement of the mobile mass has been limited by stoppers and fixed to  $z_{max}=\pm 8\text{mm}$  to limit the size of the device and to avoid buckling issues. Simulations have shown the necessity of using soft stoppers to prevent rebounds and to ensure that  $z(t)=z_{max}$  right after the shock. Moreover, experimental trials have shown the necessity of using guiding parts in order to keep oscillations on the vertical axis, avoiding the energy to be transferred in lateral resonant modes.

The mobile mass and the spring stiffness have also been optimized by simulations and should be respectively equal to  $m=130\text{g}$  and  $k=460\text{kN/m}$ . The mechanical quality factor is taken equal to 50. The electromagnetic converter is made of a NdFeB magnet and a 600-turn coil. The  $Bl$  conversion coefficient is imposed by the characteristics of the magnet, the coil and the distance between them, and has been experimentally measured at  $Bl=3.44$ . The simulated output voltage, output power and mass displacement as a function of time are presented in Figure 3.

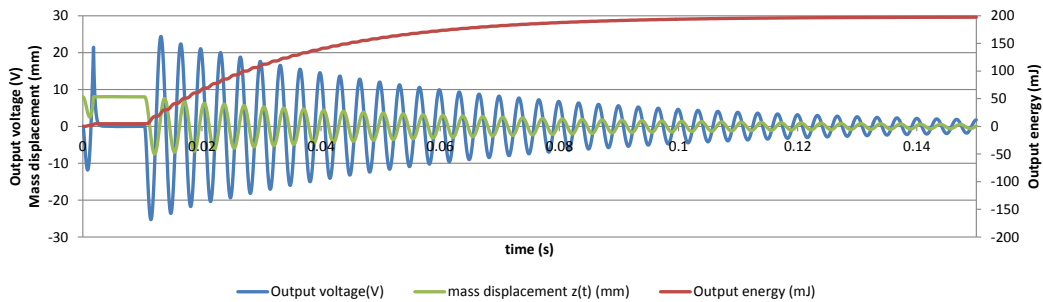


**Figure 3.** Simulated output voltage, output power and mass displacement as a function of time

### 3.2. Spring design

A double-helix spring (Figure 4) has been chosen to ensure a good stability and to better withstand buckling during the shock phase. The spring parameters have been determined by using the system of equations  $k = Gb^4/4D^3n$  and  $\tau(z_{max}) = 4K_w kz_{max}D/\pi b^3$ , where  $G$  is the shear modulus,  $D$  the mean diameter of the spring,  $b$  the wire diameter,  $n$  the number of active coils and  $K_w$  the wahl factor, to keep  $\tau(z_{max})$ , the spring stress when  $z=z_{max}$ , below 1GPa and to get  $k=460\text{kN/m}$ . Springs have been made from round steel wires, soldered on two supports (Figure 4b) and characterized in a Mecmesin 25-i traction bench (Figure 4c). The experimental spring stiffness is  $k=430\text{kN/m}$ .

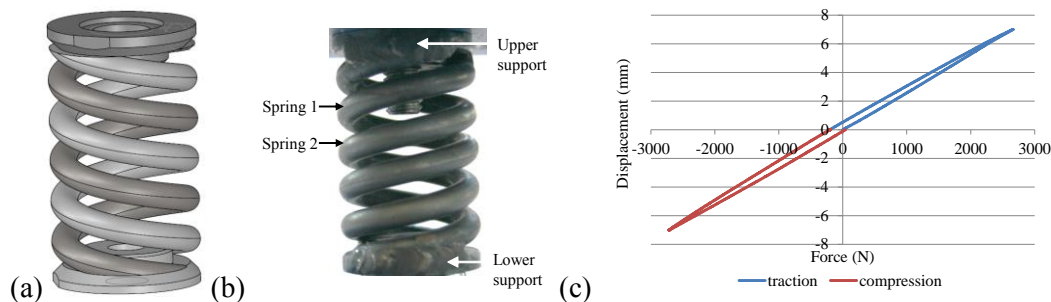


**Figure 4.** (a) Double helix spring design, (b) manufactured spring and (c) spring characterization in a traction bench (Mecmesin 25-i).



**Figure 5.** (a) Energy harvester CAD conception, (b) Prototype and (c) test bench

## 4. Manufacturing, tests and experimental results

The energy harvester has been designed in Solidworks (Figure 5a) and fabricated with standard manufacturing tools, integrating the double-helix 430kN/m spring, stoppers and guiding parts. The complete device (Figure 5b) sizes  $117\text{cm}^3$  and weighs 370g.

The system has firstly been tested in a traction bench (Mecmesin 25-i): the energy harvester is connected to a tensile jaw with a tensile specimen (Figure 5c). A stopper is used to impose the energy harvester's elongation at startup ( $z=z_{max}=8\text{mm}$ ). The tensile specimen is designed to break after the energy harvester abutted to liberate the device which enters in oscillations. The experimental resonant

frequency is  $f_{mk}=289\text{Hz}$  (Figure 6a); output voltages reach 23 volts, as predicted by simulations (Figure 3). Finally, 210mJ have been generated in 150ms (vs 200mJ targeted).

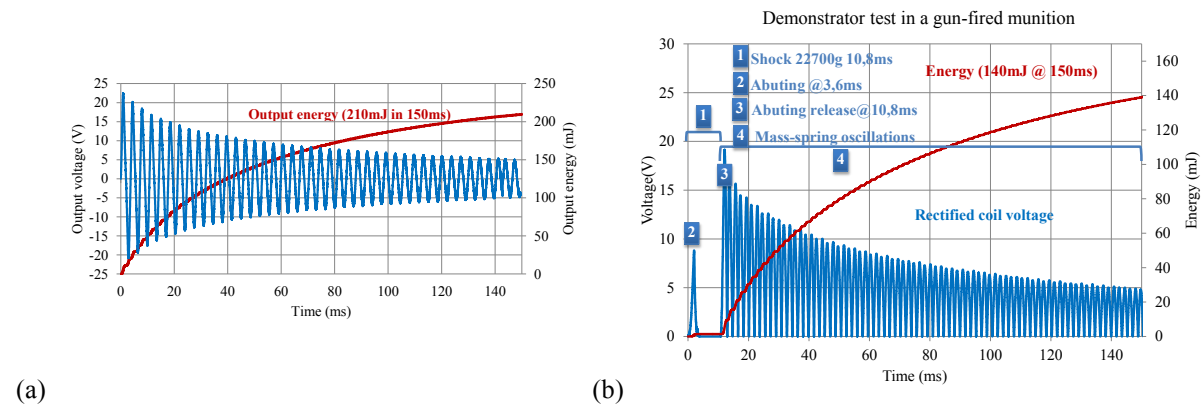


**Figure 6.** (a) Experimental output voltage and energy in the test bench – (b) In-situ tests – output voltage and output energy

The prototype was finally installed and tested in a gun-fired munition in November 2013. Experimental output voltages and energies are presented in Figure 6b: 140mJ were generated in 150ms after a 22700G shock. This corresponds to a mean output power of 0.93W and a maximum output power of 4.83W, right after the shock. The mechanical quality factor  $Q=1/(2b_m)$  was finally evaluated from experimental data and varied between  $Q=20$  right after the shock and  $Q=180$  at the end of the oscillations. Low  $Q$  is due to peripheral high stress on the springs at large displacements. Further improvements are targeted to reduce these stress and thus to increase output powers.

## 5. Conclusions

We have reported on a 20000G shock energy harvester for gun-fired munition, designed to generate 200mJ in 150ms. Prototypes have been manufactured, tested in lab and in real conditions. 210mJ have been reached in a test bench and 140mJ in a gun-fired munition, validating, for the first time, the proof of concept of 20000G shock energy harvesters for gun-fired munition exploiting an electromagnetic conversion. Output powers have reached 4.83W (41.3mW/cm<sup>3</sup>) right after the shock, one of the highest densities of power of the state of the art [7]. Research actions are now targeted towards the size reduction and the optimization of the power densities of these energy harvesters.

## References

- [1] Geisler M et al. 2016 Scaling effects of a non-linear electromagnetic energy harvester for wearable sensors, *Proc. PowerMEMS*
- [2] Boisseau S et al. 2016 Water flow energy harvesters for autonomous flowmeters, *Proc. PowerMEMS*
- [3] Rastegar J et al. 2011 Energy-Harvesting Power Sources for Gun-Fired Munitions, *Proc. SPIE 8035*
- [4] Rastegar J et al. 2006 Piezoelectric-based energy-harvesting power sources for gun-fired munitions, *Proc. SPIE 6174*
- [5] Saha C 2011 Modelling Theory and Applications of the Electromagnetic Vibrational Generator, Chapter 3: Sustainable Energy Harvesting Technologies – Past, Present and Future, *Intech*
- [6] Cheng S et al. 2007 Modeling of magnetic vibrational energy harvesters using equivalent circuit representations, *Journal of Micromechanics and Microengineering*
- [7] Moss S D et al. 2015 Scaling and power density metrics of electromagnetic vibration energy harvesting devices, *Smart Materials and Structures*